IGARSS 2024 - 2024 IEEE International Geoscience and Remote Sensing Symposium | 979-8-3503-6032-5/24/$31.00 ©2024 IEEE | DOI: 10.1109/IGARSS53475.2024.10642422

A ONE-CLASS BAYESIAN ALGORITHM FOR RADIO FREQUENCY INTERFERENCE DETECTION IN MICROWAVE RADIOMETRY

Imara Mohamed Nazar, Mustafa Aksoy

University at Albany, State University of New York, Albany, NY, USA

ABSTRACT

Measurements of Earth-observing radiometers have been reported to be contaminated by radio frequency interference (RFI) due to active emissions in the densely occupied radio spectrum. This study presents a multi-dimensional, one-class Bayesian algorithm to detect and eliminate such RFI. The proposed algorithm was trained with RFI-free measurements only and operated in a feature space where the separation between RFI-free and RFI-contaminated measurements was maximized. Using standard metrics, the performance of the Bayesian algorithm was evaluated, and it was demonstrated that the one-class detection algorithm presented in this paper can outperform the existing state-of-the-art RFI detection algorithms, specifically for the low interference to noise ratio (INR) cases.

Index Terms**—** Radio frequency interference, RFI, detection, remote sensing, microwave radiometry, Bayesian detection, one-class detection.

1. INTRODUCTION

Radio frequency interference (RFI) is an increasing threat for Earth-observing microwave radiometers as estimating important geophysical variables requires accurate and precise measurements. Along with passive services, the radio spectrum is occupied by active ones such as radars and wireless communication networks which radiate at microwave frequencies, and the frequency spectrum demand for such active services is increasing exponentially, leading to significant RFI contamination in the Earth observations [1-3]. RFI contamination causes bias in the radiometer measurements which may result in erroneous estimation of critical geophysical variables. Therefore, RFI detection and mitigation studies for microwave radiometry are of utmost importance.

Recent studies have demonstrated that machine learning algorithms can be utilized for efficient RFI detection in microwave radiometry [4-7]. Specifically, algorithms operating in multi-dimensional feature spaces which utilize only RFI-free data for their training have been proposed for cost-effective implementations [8-9]. Building upon those previous work, this study introduces a one-class Bayesian detection algorithm to identify RFI contamination in microwave radiometer measurements. Again, the proposed technique relies on only the distribution of the RFI-free measurements, a significant improvement on the Bayesian algorithms reported in [10-11], and can make statistical decisions while incorporating the uncertainties inherent in the decision-making process.

The paper first summarizes the theoretical basis of the algorithm, then evaluates its performance using simulated radiometer datasets in which RFI contamination was modeled as a pulsed-sinusoidal signal with varying duty cycle (DC) and interference to noise ratio (INR). Finally, the results are discussed in the context of implementations in real microwave radiometer deployments.

2. ONE-CLASS BAYESIAN RFI DETECTION ALGORITHM

Consider a set $\boldsymbol{r}$ of N radiometer integration windows where each window r_i, $i = \{1,2,..,N\}$, contains M number of samples and is described by d number of features, namely $F_1, F_2, \ldots, F_d$. The corresponding feature values for window r_i are denoted as f_{in}, $n = \{1,2,..,d\}$. In general, the Bayesian RFI detection is formulated as a hypothesis testing problem where each window r_i may belong to one of the two hypotheses (H_i), i.e., RFI-contaminated (H_C) and RFI-free (H_N). In one-class Bayesian detection, the problem can be formulated where r_i may belong to RFI-free (H_N) class or not. For each r_i, the posterior distribution $P(H_i|\boldsymbol{r})$ is computed via Bayes' theorem using class conditional distribution of each feature and the prior distribution of the data. To simplify the problem, the features can be assumed to be conditionally independent given the class label [12]. As a result, the final detection output, $\hat{y}_r$ is estimated using maximum a posteriori (MAP) method as follows:

$$\hat{y}_r = \arg\max P\big(H_j|\boldsymbol{r}\big),\ j = \{C, N\} \tag{1}$$

Note that the output for the detection algorithm is a probability value which models the uncertainty.

3. SIMULATED RADIOMETER MEASUREMENTS

Simulated radiometer datasets were created for the study. RFI-free radiometer measurements were modeled as white

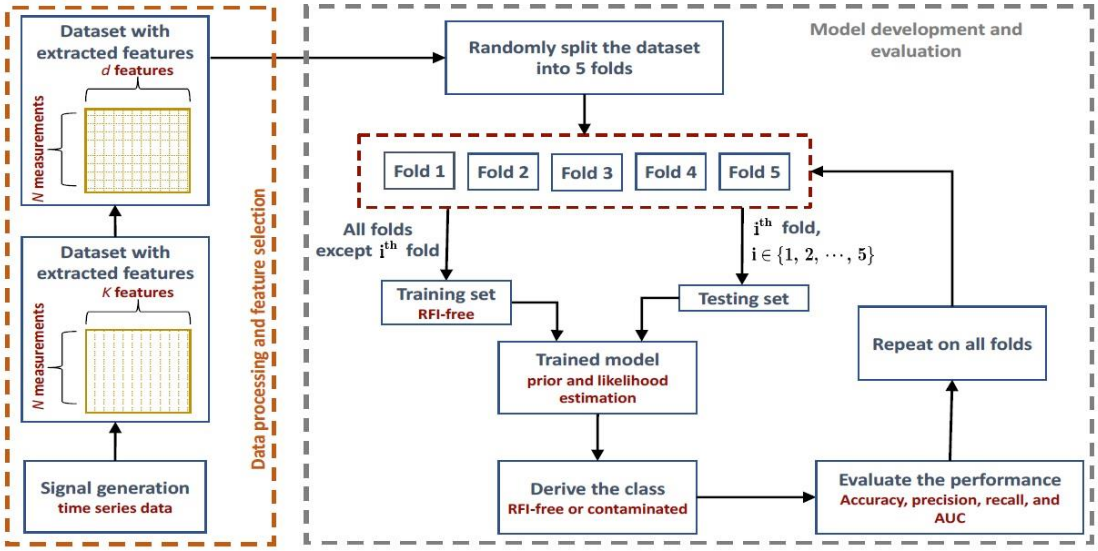

Figure 1: Implementation of the one-class Bayesian detection algorithm for this study. The process includes data generation, pre-processing, feature selection, model development, and performance evaluation.

Gaussian noise with a mean (μ) and standard deviation (σ), which can be expressed as $x_N(t) = N(\mu, \sigma^2)$. The statistical parameters, i.e., μ and σ, were set to 0 V and 8 V, respectively and the sampling rate was accepted to be 75 MSPS as empirically calculated from the Soil Moisture Active Passive Validation Experiment 2012 (SMAPVEX12) airborne data measured by the Passive Active L-Band System (PALS) [13].

On the other hand, the interference was assumed to be a pulsed-sinusoidal signal with varying DC and INR, and RFI-contaminated radiometer observations were simulated by adding such interference to the RFI-free measurements. Thus, RFI-contaminated radiometer measurements could be expressed as:

$$x_C(t) = x_N(t) + A\,sin(2\pi f t + \varphi)rect\left(\frac{t-t_0}{\omega}\right) \quad (2)$$

where A, f, and φ denote the amplitude, frequency, and phase shift of the interference signal. The $rect()$ function provided a rectangular pulse envelope which determined DC, and t_0 and ω controlled the time delay and width of the envelope, respectively. In particular, ω could be written in terms of the DC of the interference signal and the radiometer integration period (T) as $DC = {}^{\omega}/_{T}$. The value of T, the length of each radiometer integration window, was set to 350 μs, again similar to the PALS radiometer [13]. The variable parameters (A, f, and φ) were assumed to be uniformly distributed in their respective ranges. f was varied uniformly within the the PALS intermediate frequency (IF) band, from 15 MHz to 35 MHz. φ was also taken as a uniformly distributed random variable between 0 and 2π radians. Finally, A was varied to create the RFI contamination with INR values from -20 dB to 10 dB, and DC was changed from 1% to 100%. Overall, three thousand one hundred RFI contaminated radiometer integration windows with distinct INR and DC values were generated.

To better reveal the characteristics of the simulated time series radiometer data, they were translated to a heterogeneous feature space, where each radiometer integration window was represented with thirty-one temporal, statistical, spectral features listed in [8].

4. IMPLEMENTATION OF THE ALGORITHM

To reduce the computational complexity of the algorithm, a feature selection algorithm, first introduced in [8], was applied as the first step of RFI detection. The relevant subset of features which would increase the separability between the RFI-free and the RFI-contaminated radiometer measurements were identified as the variance, power, average over absolute value of first differences, mean of the auto-correlation coefficient, power spectral maximum, spectral entropy, spectral skewness, spectral kurtosis, spectral crest, spectral flatness, and spectral flux.

Implementation of the Bayesian detection is illustrated in Figure 1. After RFI-free and RFI-contaminated radiometer measurements were generated and the relevant features were identified, the features were organized in rows to construct the data matrix. The data matrix was divided into two parts for training and testing. The training data, RFI-free as previously mentioned, was used to train the Bayesian detection model which outputs the training parameters such as prior and likelihood probabilities using maximum likelihood estimation. Then, the trained Bayesian detection model was evaluated on the test data to assess the algorithm performance. To avoid overfitting, a five-fold cross-validation was implemented during which the data matrix

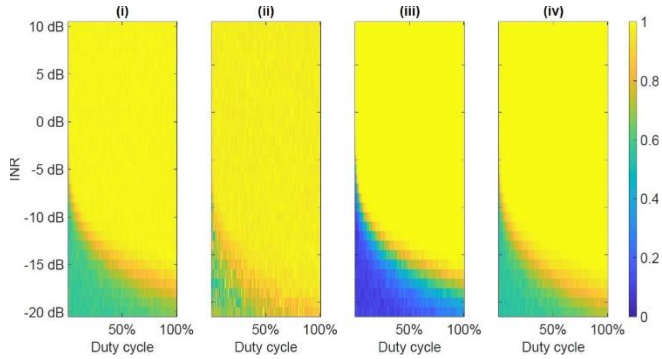

Figure 2: (i) Accuracy, (ii) precision, (iii) recall, and (iv) AUC values for one-class Bayesian RFI detection algorithm as functions of the INR and DC of the RFI-contaminated radiometer measurements.

was divided into five folds of approximately equal size where each fold was treated as a validation set for the model trained on the remaining four-folds.

5. PERFORMANCE ANALYSES

Accuracy, precision, recall, and area under the curve (AUC) were used as metrics to quantitatively evaluate the performance of the one-class Bayesian algorithm against pulsed-sinusoidal RFI. Accuracy denotes the ratio of correctly identified, as RFI-free or RFI-contaminated, measurements to the total number of measurements. Precision provides the ratio of correctly identified RFI-contaminated measurements to the total number of the measurements identified as RFI-contaminated. Note that some of the RFI-free measurements can be falsely identified as RFI-contaminated. Finally, recall is the ratio of correctly identified RFI-contaminated measurements to the total number of truly RFI-contaminated measurements. Accuracy, precision, and recall metrics can be mathematically defined as follows:

$$\begin{gathered} Accuracy = \frac{TP+TN}{TP+FP+TN+FN} \\ Precision = \frac{TP}{TP+FP} \\ Recall = \frac{TP}{TP+FN} \end{gathered} \tag{3}$$

where TP is the number true positives, i.e., number of RFI-contaminated measurements identified as RFI-contaminated, TN is the number of true negatives, i.e., number of RFI-free measurements identified as RFI-free, FP is the number of false positives, i.e., number of RFI-free measurements identified as RFI-contaminated, and FN is the number of false negatives, i.e., number of RFI-contaminated measurements identified as RFI-free. AUC, computed using the receiver operating characteristics (TP vs FP) curve, on the other hand, was used to quantify the overall performance of the proposed detection algorithm.

Performance metrics in (3) were calculated for all the three thousand one hundred RFI cases with different INR and DC levels after implementing the detection algorithm. Figure 2 shows their values as functions of INR and DC. It can be seen from the figure that nearly perfect accuracy, precision, recall, and AUC have been achieved for INR levels as low as -10 dB. This performance can also be extended to even lower INR levels if the DC is high enough.

6. CONCLUSIONS AND DISCUSSION

In this study, a feature-based, multi-dimensional, one-class Bayesian detection algorithm trained with only RFI-free measurements is introduced and analyzed for detecting pulsed-sinusoidal RFI in microwave radiometer measurements. The performance analyses have suggested efficient detection for INR cases as low as -20 dB provided that DC values are high. Even for low DC levels, the algorithm can detect interference contamination if INR is higher than -10 dB. Therefore, it can be stated that the proposed one-class Bayesian detection algorithm outperforms the state-of-the-art RFI detectors such as pulse blanking and kurtosis methods in terms of accuracy, precision, recall, and AUC metrics, especially at low INR levels [8].

Note that even though the one-class algorithm requires prior information regarding the RFI-free radiometer measurements for training, this can be collected during remote sensing missions, from presumably RFI-free zones with minimal human activity such as forests, vegetation lands, deserts, ocean surfaces, ice sheets, etc.

Future research will include identifying globally robust features that can provide better separation between RFI-free and RFI-contaminated measurements for various RFI types (other than pulsed-sinusoidal) representing the dynamic RFI environment. Furthermore, the novel RFI detection algorithm will be applied to real radiometer data, and possible training and learning mechanisms for such algorithms during actual remote sensing operations will be studied.

7. ACKNOWLEDGMENT

This material is based upon work supported by the National Science Foundation under grant number 2143592.

8. REFERENCES

[1] Aksoy, Mustafa, Hamid Rajabi, Pranjal Atrey, and Imara Mohamed Nazar. "Characteristics of the global radio frequency interference in the protected portion of L-band." *Remote Sensing* 13, no. 2 (2021): 253.

[2] Piepmeier, Jeffrey R. "RFI problems and solutions in spaceborne microwave radiometers." *Proc. 29th URSI Gen. Assembly* (2008): 7-16.

[3] Misra, Sidharth, and Paolo de Matthaeis. "Passive remote sensing and radio frequency interference (RFI): An overview of spectrum allocations and RFI management algorithms [technical committees]." *IEEE Geoscience and Remote Sensing Magazine* 2, no. 2 (2014): 68-73.

[4] Nazar, Imara Mohamed, and Mustafa Aksoy. "Radio Frequency Interference Detection in Microwave Radiometry Using Density Based Spatial Clustering." In *2021 XXXIVth General Assembly and Scientific Symposium of the International Union of Radio Science (URSI GASS)*, pp. 1-4. IEEE, 2021.

[5] Aksoy, Mustafa, and Imara Mohamed Nazar. "A Multi-Dimensional Radio Frequency Interference Detection Algorithm for Microwave Radiometry." In *IGARSS 2022-2022 IEEE International Geoscience and Remote Sensing Symposium*, pp. 5278-5281. IEEE, 2022.

[6] Mohammed, Priscilla N., and Jeffrey R. Piepmeier. "Microwave radiometer RFI detection using deep learning." *IEEE Journal of Selected Topics in Applied Earth Observations and Remote Sensing* 14 (2021): 6398-6405.

[7] Alam, Ahmed Manavi, Mehmet Kurum, and Ali C. Gurbuz. "Radio Frequency Interference Detection for SMAP Radiometer Using Convolutional Neural Networks." *IEEE Journal of Selected Topics in Applied Earth Observations and Remote Sensing* 15 (2022): 10099-10112.

[8] Nazar, Imara Mohamed, and Mustafa Aksoy. "Radio Frequency Interference Detection in Passive Microwave Remote Sensing Using One-Class Support Vector Machines." *IEEE Journal of Selected Topics in Applied Earth Observations and Remote Sensing* (2023).

[9] Nazar, Imara Mohamed, and Mustafa Aksoy. "Radio Frequency Interference Detection in Microwave Radiometry Using Multi–Dimensional Semi Supervised Learning." In *IGARSS 2023-2023 IEEE International Geoscience and Remote Sensing Symposium*, pp. 589-591. IEEE, 2023.

[10] Nazar, Imara Mohamed, and Mustafa Aksoy. "Radio Frequency Interference Detection in Microwave Radiometry: A Novel Feature-Based Statistical Approach." In *2022 3rd URSI Atlantic and Asia Pacific Radio Science Meeting (AT-AP-RASC)*, pp. 1-4. IEEE, 2022.

[11] Nazar, Imara Mohamed, and Mustafa Aksoy. "Radio Frequency Interference Detection in Microwave Radiometry Using Bayesian Detection." In *2022 United States National Committee of URSI National Radio Science Meeting (USNC-URSI NRSM)*, pp. 249-250. IEEE, 2022.

[12] Murphy, Kevin P. *Machine learning: a probabilistic perspective*. MIT press, 2012.

[13] Aksoy, Mustafa, Joel T. Johnson, Sidharth Misra, Andreas Colliander, and Ian O'Dwyer. "L-band radio-frequency interference observations during the SMAP validation experiment 2012." *IEEE Transactions on Geoscience and Remote Sensing* 54, no. 3 (2015): 1323-1335.